Available online at www.sciencedirect.com
SCIENCE DIRECT®
Journal of Power Sources 125 (2004) 119–123
JOURNAL OF POWER SOURCES
www.elsevier.com/locate/jpowsour

Short communication

Effect of reaction media on electrochemical performance of nanocrystalline manganese oxyiodides prepared by *Chimie Douce* route

Seong-Ju Hwang [a,*], Dae-Hoon Park [a], Chai-Won Kwon [b], Guy Campet [b], Jin-Ho Choy [c,1]

[a] *Department of Applied Chemistry, Chungju Campus, College of Natural Sciences, Konkuk University, Chungju 380-701, South Korea*
[b] *Institut de Chimie de la Matiére Condensée de Bordeaux (ICMCB) du CNRS, Avenue du Dr. Schweitzer 87, 33608 Pessac, France*
[c] *National Nanohybrid Materials Laboratory, School of Chemistry, Seoul National University, Seoul 151-747, South Korea*

Received 2 June 2003; received in revised form 25 July 2003; accepted 25 July 2003

Abstract

Anhydrous alkali metal-based manganese oxyiodide nanocrystals have been prepared by reduction of permanganate with LiI in acetone solvent, and their electrochemical properties have been characterized in comparison with hydrous homologues synthesized in aqueous solution. According to X-ray diffraction analysis, all the present manganese oxyiodides show no distinct (*h k l*) reflections. This indicates the nanocrystalline nature of the materials. Electrochemical measurements reveal that the anhydrous samples have a large initial discharge capacity of >300 mAh g^{-1} at a constant current density of 0.2 mA cm^{-2}, which is comparable with the capacities of hydrous samples. Despite the absence of lattice water, however, the manganese oxyiodides suffer from greater capacity loss than the water-containing nanocrystals. According to the differential capacity plot, it is clear that the structural stability of the anhydrous nanocrystals is much poorer than that of the hydrous ones. Given that the iodine species helps to maintain the nanocrystalline nature of the electrode materials, the significant capacity loss for the anhydrous nanocrystals can be explained in terms of structural instability caused by the low concentration of iodine species.

Keywords: Nanocrystals; Capacity loss; Iodine species; Structural stability; Differential capacity; Lithium battery

1. Introduction

Intercalation electrodes for lithium secondary batteries have been studied extensively for several decades [1,2]. Until now, the most successfully commercialized cathode material is layered $LiCoO_2$ which has several advantages such as electrochemical stability, small capacity loss, and ease of synthesis [3]. Nevertheless, the high price and high toxicity of cobalt evokes research efforts to develop new cathode materials. In this regard, special attention has been paid to the development of cheap and non-toxic manganese- or iron-containing compounds such as spinel $LiMn_2O_4$, layered $LiMnO_2$, and olivine $LiFe_{1-x}Mn_xPO_4$, etc. [4–13]. Many of the candidate materials suffer from capacity decrease during extended electrochemical cycling. Such a problem is attributed to phase transition of the crystal structure during the lithium intercalation–disintercalation reaction [7,14]. Recently, it has been reported [15–18] that nanocrystalline materials are much more tolerable for the repeated Li insertion–extraction process. For example, we have found that nanocrystalline spinel lithium manganate exhibits enhanced electrochemical performance in the 3-V region, which corresponds to Li insertion into the 16c site. This can be understood in terms of the grafting mechanism of lithium on the surface of nanocrystalline materials [19].

Another advantage of nanocrystalline materials is that they can be prepared by environmentally benign and less energy-consuming *Chimie Douce* reactions. The term *Chimie Douce* describes 'soft chemistry' by which the solid-state compound is formed under milder conditions such as redox, hydrothermal, and intercalation reactions below 300 °C. With this synthesis method, it is easy to scale up the amount of products for mass production. By virtue of such attributes, nanocrystalline compounds have attracted considerable interest as electrode materials.

Very recently, we have prepared potassium-based manganese oxyiodide by reacting an aqueous solution of potassium permanganate and LiI, and found that this material shows a large initial capacity up to ~340 mAh g^{-1} at a constant current density of 0.2 mA cm^{-2} [20]. Unfortunately,

* Corresponding author. Tel.: +82-43-840-3569; fax: +82-43-851-4169.
E-mail address: hwangsju@kku.ac.kr (S.-J. Hwang).
[1] Co-corresponding author.

0378-7753/$ – see front matter © 2003 Elsevier B.V. All rights reserved.
doi:10.1016/j.jpowsour.2003.07.012

the use of aqueous reaction media gives rise to capacity fading with charge–discharge cycling, which is attributable to the reaction between lattice water and $LiPF_6$ salt in electrolyte [21]. Actually, Na-based manganese oxyiodide prepared in acetonitrile shows better capacity retention than the water-containing homologue [15]. On the other hand, the toxicity of acetonitrile plagues the large-scale preparation of this nanocrystalline material. In this regard, alternative solvents to acetonitrile have been sought. Although most polar organic solvents are oxidized readily by permanganate, acetone is found to be relatively stable for oxidation and less toxic than acetonitrile. For this reason, we have adopted acetone as the reaction media for preparing anhydrous manganese oxyiodides. The physico-chemical properties of these compounds have been compared with those of hydrous homologues, in order to investigate the effect of solvent on the phase stability and the electrochemical performance of nanocrystalline materials.

2. Experimental

The anhydrous K–Li–Mn–O–I (KA) and Na–Li–Mn–O–I (NA) samples were prepared by reacting an acetone solution of $KMnO_4$ or $NaMnO_4$ with 1.5 equiv. LiI at room temperature. $NaMnO_4$ was obtained by heating $NaMnO_4{\cdot}H_2O$ at 170 °C for 2 h under vacuum, whereas $KMnO_4$ was used as received. The mixed solution was maintained at room temperature for 1 day under constant stirring. The resulting precipitate was washed with acetone and methanol, and dried at 80 °C under vacuum. Chemical lithiation for these samples was carried out by reaction with 1.6 M *n*-BuLi in hexane for 48 h. Prior to the physico-chemical characterization, the lithiated samples were washed thoroughly with hexane and dried in vacuum. For comparison, both K- and Na-based nanocrystalline samples were also prepared by reacting an aqueous solution of $KMnO_4$ or $NaMnO_4$ with 1.5 equiv. LiI at room temperature (KW and NW). To minimize the amount of lattice water, the resulting powders were vacuum-dried at 130 °C overnight.

The crystal structure of manganese oxyiodides and their chemically lithiated products was examined by X-ray diffraction (XRD) using Ni-filtered Cu Kα radiation with a graphite diffracted beam monochromator. The chemical compositions of the samples were determined by means of atomic absorption (AA) spectrometry, inductive coupled plasma (ICP) spectrometry, thermogravimetric analysis (TGA), and electron probe micro-analysis (EPMA).

Electrochemical measurements were performed with the cell configuration of Li|1 M $LiPF_6$ in EC:DMC (50:50 v/v)|composite cathode, which was assembled in a dry box. The composite cathode was prepared by mixing thoroughly the active manganese oxyiodide material (70 wt.%) with 25 wt.% of acetylene black and 5 wt.% of polytetrafluoroethylene (PTFE). All experiments were performed in a galvanostatic mode with an Arbin BT 2043 multichannel galvanostat/potentiostat in the voltage range 1.5–4.3 V at a constant current density of 0.2 mA cm^{-2}.

3. Results and discussion

Powder XRD patterns of the anhydrous nanocrystals (KA and NA) are shown in Fig. 1, together with those of their heated and lithiated derivatives. The corresponding data of KW and NW are not shown here, since the overall spectral features are nearly the same as those of the present anhydrous samples [20]. All the anhydrous manganese oxyiodides display no distinct XRD, which indicates the nanocrystalline nature of the samples. After the heat-treatment at 600 °C, an amorphous phase is changed into a mixed crystalline phase, that is, a mixture of rhombohedral layered K_xMnO_2 and Li-rich Li_2MnO_3 for KA, and a mixture of $Na_{0.7}MnO_2$ and Li-rich Li_2MnO_3 for NA. This is in contrast with the cases of KW and NW in which the mixture of cubic-spinel $Li_{1+y}Mn_{2-y}O_4$ and the layered A_xMnO_2 (A = K, Na) are formed after heat treatment [20]. Such a difference is most likely due to the dissimilar lithium contents in the pristine nanocrystals. The lithiated derivatives of anhydrous KA and NA do not exhibit any sharp XRD peaks related to crystalline lithium manganate or lithium hydroxide. This observation differs from that for hydrous KW and NW which exhibit several weak reflections that correspond to lithium hydroxide hydrate formed by a reaction with *n*-BuLi and lattice water [20]. Thus, it is concluded that the anhydrous compounds prepared in acetone do not possess any lattice water.

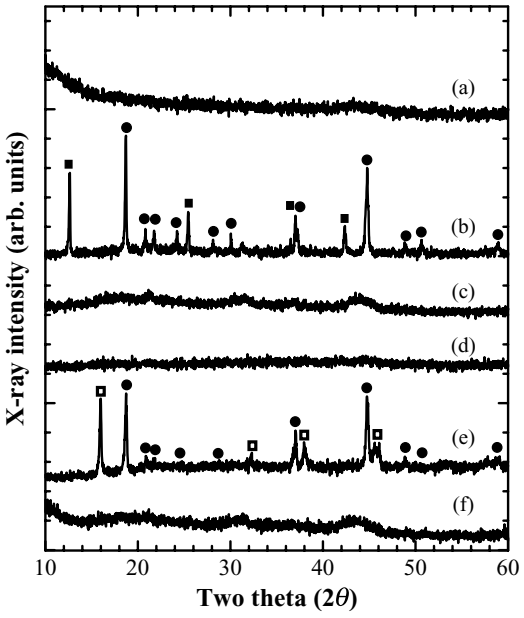

Fig. 1. X-ray diffraction patterns of nanocrystalline alkali metal-based manganese oxyiodide: (a) KA, (b) KA after the heat-treatment at 600 °C, (c) KA after lithiation, (d–f) corresponding data for NA. In (b) and (e), symbols (●, ■, □) represent the reflections from Li_2MnO_3, $K_xMnO_2{\cdot}yH_2O$, and $Na_{0.7}MnO_2$ phases, respectively.

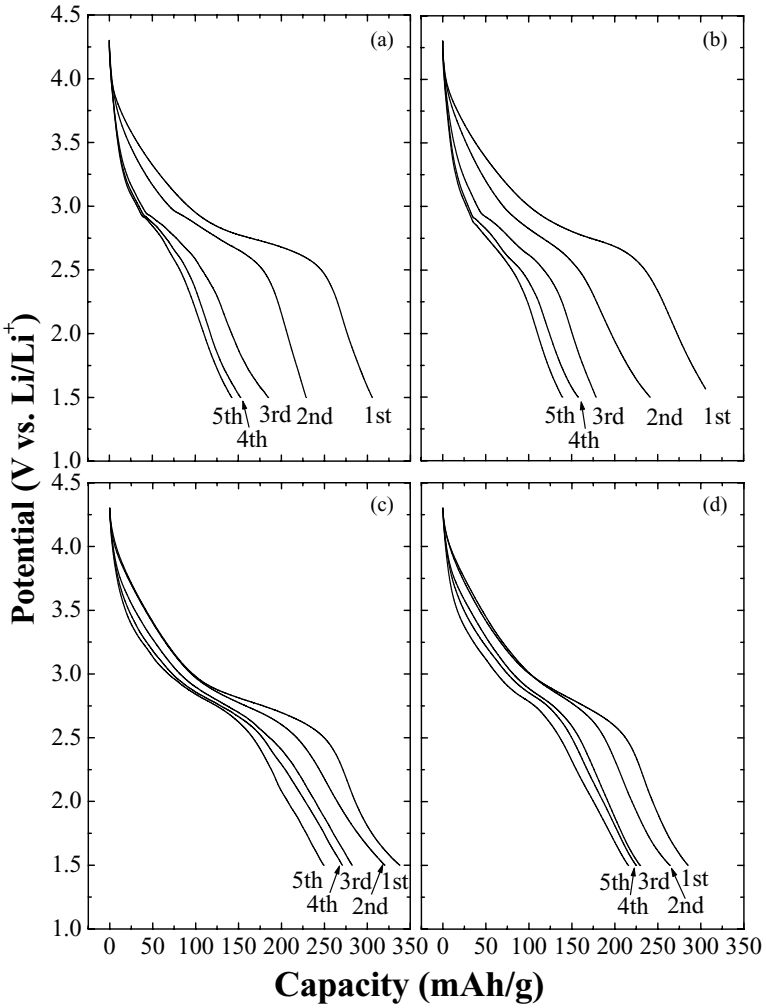

Fig. 2. Discharge potential profiles of nanocrystalline alkali metal-based manganese oxyiodides: (a) KA, (b) NA, (c) KW, (d) NW.

The chemical formulae of the nanocrystalline compounds (KA, NA, KW, NW) and their lithiated derivatives estimated from AA, ICP, and EPMA analyses are summarized in Table 1. The concentration of alkali metal ion is determined to be higher for the anhydrous nanocrystals than for the hydrous ones, whereas the iodine content is lower for the former compared with the latter. It is also found that the difference of alkali metal concentration between the anhydrous and the hydrous samples increases in the order of K < Na < Li. Such a variation of stoichiometry can be understood from the dissimilar solubility of alkali metal ions and iodine for acetone and water. That is, alkali metal ion is well dissolved in water compared with acetone, which leads to a lower content of alkali metal in the precipitate (i.e. the hydrous nanocrystals). Actually, the solubility for water increases in the order KI < NaI < LiI, whereas that for acetone decreases in this order [22]. This is in good agreement with the trend in the concentration difference of alkali metal ion. On the other hand, iodine is more effectively dissolved in acetone than in water, which results in a smaller concentration of iodine in the anhydrous samples. As shown in Table 1, the lithiation process generally causes the incorporation of about two moles of lithium ions per unit formula in all the present nanocrystalline materials. This reflects their greater ability to accommodate lithium ions compared with well-crystallized electrode materials such as $LiMn_2O_4$ spinel.

Table 1
Chemical formulae of nanocrystalline manganese oxyiodides and the lithiated derivatives

Sample	As prepared	Lithiated
KA	$Li_{1.28}K_{0.36}MnO_{3.0-\delta}I_{0.03}$	$Li_{3.12}K_{0.40}MnO_{3.0-\delta}I_{0.03}$
NA	$Li_{1.40}Na_{1.34}MnO_{3.0-\delta}I_{0.03}$	$Li_{3.34}Na_{0.91}MnO_{3.0-\delta}I_{0.03}$
KW[a]	$Li_{0.54}K_{0.3}MnO_{3.0-\delta}I_{0.10}$	$Li_{2.45}K_{0.34}MnO_{3.0-\delta}I_{0.13}$
NW[a]	$Li_{0.52}Na_{0.62}MnO_{3.0-\delta}I_{00.7}$	$Li_{2.48}Na_{0.79}MnO_{3.0-\delta}I_{0.08}$

[a] From TGA results, the water content of the hydrous nanocrystals was determined to be about 0.2–0.4 mole water per unit formula.

The cycling characteristics of alkali metal-based manganese oxyiodides have been examined to examine the effect of reaction media on the electrochemical performance of these nanocrystalline materials.[2] The open-circuit poten-

[2] The present electrochemical data were obtained from NA and KA after heating at 80 °C under vacuum. The samples dried at higher temperature (>130 °C) show a slightly poorer electrochemical performance.

tial (OCV) of the anhydrous samples (KA and NA) is determined to be about 3.26–3.28 V (vs. Li/Li^+), which is slightly lower than that of the hydrous counterparts (KW and NW) about 3.43–3.46 V (vs. Li/Li^+). The smaller OCV value for the anhydrous samples implies a lower oxidation state for manganese, which would be related to the higher content of alkali metal cation.

The discharge potential profiles of KA and NA are presented in Fig. 2, together with those of KW and NW. All the present nanocrystals display nearly the same initial discharge behavior, which is very close to that previously reported for nanocrystalline manganese oxide [21]. This can be regarded as evidence for the nanocrystalline character of the pristine manganese oxyiodides. Such a smooth decrease of potential during the discharge process has been reported [23,24] for nanocrystalline electrode materials such as SnO_2 and Fe_2O_3. In terms of band structure, this phenomenon can be explained by the formation of many sub-bands between the valence and conduction bands caused by the existence of surface defects and/or surface dangling bonds in nanocrystalline materials, which lead to a smooth change in Fermi-energy and, hence a moderate potential change upon Li insertion [19].

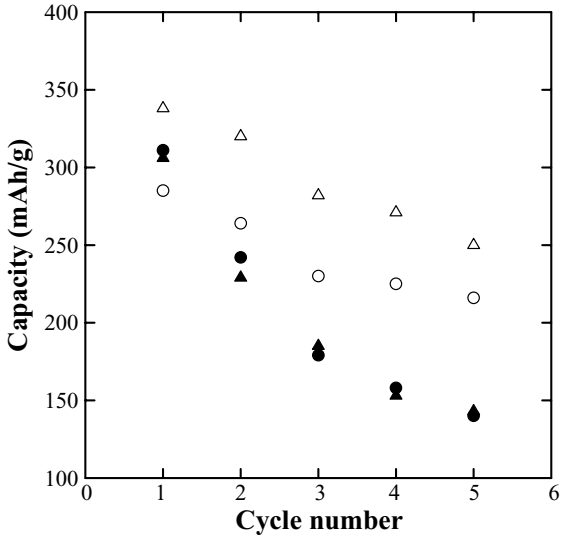

Fig. 3. Discharge capacities of nanocrystalline alkali metal-based manganese oxyiodides: KA (▲), NA (●), KW (△), NW (○).

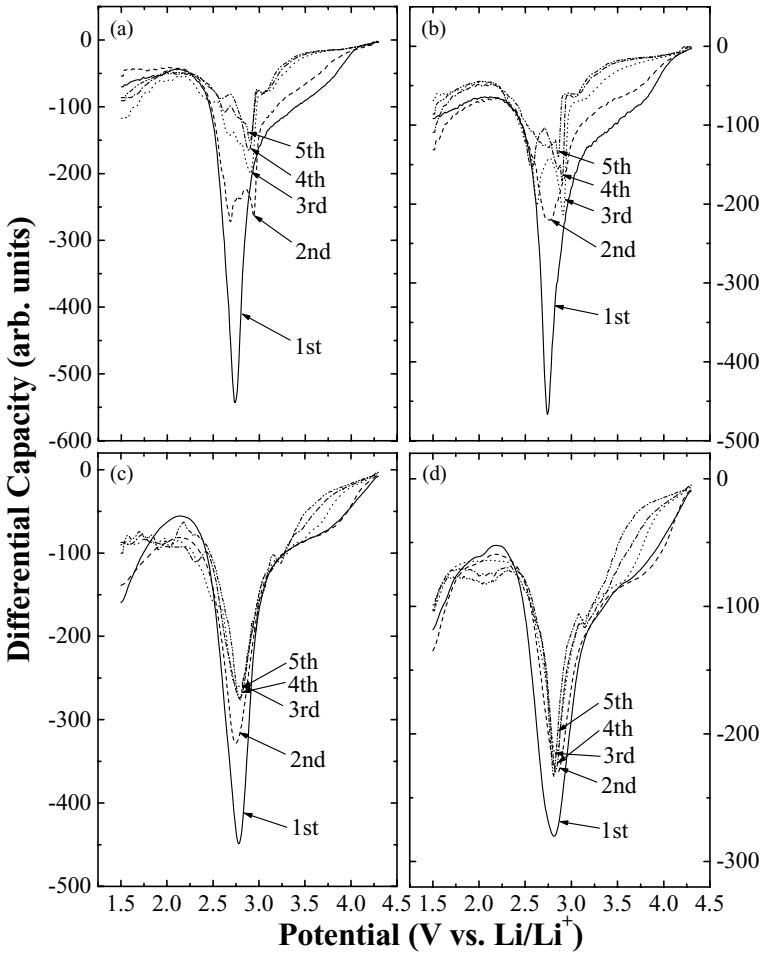

Fig. 4. Differential capacity profiles of nanocrystalline alkali metal-based manganese oxyiodides: (a) KA, (b) NA, (c) KW, (d) NW.

The discharge capacities of the anhydrous KA and NA compounds are displayed in Fig. 3 as a function of cycle number, and are compared with those of the hydrous KW and NW compounds. Even though there is no lattice water in the anhydrous samples, a more prominent capacity fading is observed for these materials compared with hydrous nanocrystals. This is in disagreement with previous results for the anhydrous manganese oxyiodide prepared in acetonitrile media [15]. For the purpose of understanding this unexpected result, the variation in discharge profiles was examined in detail by plotting the differential capacity profiles for KA and NA, together with those for KW and NW, see Fig. 4 In contrast to the hydrous KW and NW samples which show only a small variation, both anhydrous KA and NA samples exhibit obvious splitting of the single peak at 2.7 V into two or three features with progressive electrochemical cycling. Given that each peak in the differential capacity plot represents a specific Mn site, the observed spectral change indicates that the crystal structure of the anhydrous samples is markedly modified by the Li intercalcation–disintercalation process, and hence several different Mn sites are created. Therefore, it is quite clear that the structural stability of the anhydrous samples is much poorer than that of the hydrous counterparts.

Raman results have shown [20] that the manganese ion in alkali-based manganese oxyiodides is stabilized in the octahedral site of rhombohedral layered lattice. It is well-known that the layered lithium manganate experiences a structural transition to the spinel-type cation ordering upon electrochemical cycling [7,25]. As indicated by the negligible variation in the differential capacity plot (Fig. 4), hydrous KW and NW nanocrystals do not show such a structural transition. This can be explained by the fact that nanocrystalline materials are more tolerable of Li insertion–extraction and are, therefore, more stable towards structural modification [15–18]. More importantly, the presence of iodine species on the surface and at the grain boundaries helps to maintain the nanocrystalline nature, and hence enhances the structural stability of the materials [20]. In comparison with the hydrous samples NW and KW, the anhydrous nanocrystals NA and KA possess lower iodine content and poorer structural stability during the electrochemical cycling process, as evidenced by the differential capacity plot (Fig. 4). Thus, it can be concluded that the poor electrochemical performance of the anhydrous nanocrystals is due to the low content of iodine species. In fact, it has been reported that the Na-based manganese oxyiodide with a high iodate content (0.15 iodine per manganese) shows excellent electrochemical performance without capacity fading [15]. Finally, it is very important to select a proper reaction media for optimizing the electrochemical performance of nanocrystalline electrode materials prepared by the *Chimie Douce* route. X-ray absorption and micro-Raman spectroscopic studies of these compounds are in progress in order to understand fully the effect of reaction media on the chemical bonding nature of nanocrystalline materials.

Acknowledgements

This work was supported by Konkuk University in 2003 and in part by the Ministry of Sciences and Technology through NRL project 1999.

References

[1] K. Mizushima, P.C. Jones, P.J. Wiseman, J.B. Goodenough, Mater. Res. Bull. 15 (1980) 783.
[2] M.M. Thackeray, P.J. Johnson, L.A. de Piccioto, P.G. Bruce, J.B. Goodenough, Mater. Res. Bull. 19 (1984) 179.
[3] T. Nagaura, K. Tazawa, Prog. Batteries Solar Cells 9 (1990) 20.
[4] M.M. Thackeray, Prog. Solid. State. Chem. 25 (1997) 1.
[5] A.R. Armstrong, P.G. Bruce, Nature 381 (1996) 499.
[6] F. Capitaine, P. Gravereau, C. Delmas, Solid State Ionics 89 (1996) 197.
[7] S.J. Hwang, H.S. Park, J.H. Choy, G. Campet, Chem. Mater. 12 (2000) 1818.
[8] S.J. Hwang, H.S. Park, J.H. Choy, G. Campet, J. Phys. Chem. B 104 (2000) 7612.
[9] H.S. Park, S.J. Hwang, J.H. Choy, J. Phys. Chem. B 105 (2001) 4860.
[10] S.J. Hwang, H.S. Park, J.H. Choy, G. Campet, J. Phys. Chem. B 104 (2001) 335.
[11] A.K. Padhi, K.S. Nanjundaswamy, J.B. Goodenough, J. Electrochem. Soc. 144 (1997) 1188.
[12] A. Yamada, Y. Kudo, K.Y. Liu, J. Electrochem. Soc. 148 (2001) A1153.
[13] F. Croce, A.D. Epifanio, J. Hassoun, A. Deptula, T. Olczac, B. Scrosati, Electrochem. Solid-State Lett. 5 (2002) A47.
[14] R.J. Gummow, D.C. Liles, J.B. Goodenough, Mater. Res. Bull. 28 (1993) 1249.
[15] J. Kim, A. Manthiram, Nature 390 (1997) 265.
[16] A. Manthiram, J. Kim, Chem. Mater. 10 (1998) 2895.
[17] J. Kim, A. Manthiram, Electrochem. Solid-State Lett. 2 (1999) 55.
[18] C.R. Horne, U. Bergmann, J. Kim, K.A. Striebel, A. Manthiram, S.P. Cramer, E.J. Cairns, J. Electrochem. Soc. 147 (2000) 395.
[19] N. Treuil, C. Labrugère, M. Menetrier, J. Portier, G. Campet, A. Deshayes, J.C. Frison, S.J. Hwang, S.W. Song, J.H. Choy, J. Phys. Chem. B 103 (1999) 2100.
[20] S.J. Hwang, C.W. Kwon, J. Portier, G. Campet, H.S. Park, J.H. Choy, P.V. Huong, M. Yoshimura, M. Kakihana, J. Phys. Chem. B 106 (2002) 4053.
[21] J.J. Xu, A.J. Kinser, B.B. Owens, W.H. Smyrl, Electrochem. Solid-State Lett. 1 (1998) 1.
[22] J.E. Huheey, E.A. Keiter, R.L. Keiter, Inorganic Chemistry: Principles of Structure and Reactivity, fourth edn., HarperCollins College Publisher, New York, 1993, pp. 312–314.
[23] C.W. Kwon, G. Campet, J. Portier, A. Poquet, L. Fournes, C. Labrugere, B. Jousseaume, T. Toupance, J.H. Choy, M.A. Subramanian, Int'l. J. Inorg. Mater. 3 (2001) 211.
[24] G. Campet, S.J. Wen, S.D. Han, M.C.R. Shastry, J. Portier, C. Guizard, L. Cot, Y. Xu, J. Salardennet, Mater. Sci. Eng. B 18 (1993) 201.
[25] Y. Shao-Horn, S.A. Hackney, A.R. Armstrong, P.G. Bruce, R. Gitzendanner, C.S. Johnson, M.M. Thackeray, J. Electrochem. Soc. 146 (1999) 2404.